Polymer 50 (2009) 211–217

Contents lists available at ScienceDirect

Polymer

journal homepage: www.elsevier.com/locate/polymer

Self-assembly of ethyl cellulose-*graft*-polystyrene copolymers in acetone

Wenyong Liu [a,b], Ruigang Liu [a,*], Yanxiang Li [a,b], Hongliang Kang [a,b], Dawa Shen [a,b], Min Wu [a], Yong Huang [a,c,*]

[a] *State Key Laboratory of Polymer Physics and Chemistry, Joint Laboratory of Polymer Science and Materials, Beijing National Laboratory for Molecular Sciences (BNLMS), Institute of Chemistry, Chinese Academy of Sciences, Beijing 100190, China*

[b] *Graduate University, Chinese Academy of Sciences, Beijing 100039, China*

[c] *Laboratory of Cellulose and Lignocellulosics Chemistry, Guangzhou Institute of Chemistry, Chinese Academy of Sciences, Guangzhou 510650, China*

ARTICLE INFO

Article history:
Received 28 March 2008
Received in revised form
22 October 2008
Accepted 31 October 2008
Available online 18 November 2008

Keywords:
Dense graft copolymer
Ethyl cellulose
Self-assembly

ABSTRACT

The self-assembly of the dense graft copolymers ethyl cellulose-*graft*-polystyrene (EC-*g*-PS) in acetone was investigated by using dynamic light scattering (DLS), transmission electron microscopy (TEM) and scanning electron microscopy (SEM). It was found that EC-*g*-PS copolymers can self-assemble into spherical micelles in acetone. The micelles' size increases with increasing the copolymer concentration and the PS side-chain length. Moreover, the copolymers can self-assemble into multimolecular micelles at relatively high polymer concentration while unimolecular micelles can be formed at low concentration. The micelles have a core–shell structure with the ethyl cellulose main chains in the shell and the side polystyrene chains in the core of the micelles.

1. Introduction

The self-assembly of block and graft copolymers has received increasing interest for their potential applications in many fields, such as drug carriers, and had been studied extensively from both theoretical and experimental aspects [1–6]. Block and graft copolymers can form micelles in selective solvents, which are thermodynamically a good solvent for one of the components and comparatively a poor solvent for the other [7]. The micelles of block or graft copolymers are formed by molecular associations [8]. Intramolecular association will lead to the unimolecular micelles, while inter-molecular association will lead to the multimolecular micelles [9–15]. Compared with block copolymers, graft copolymers are much easier to form unimolecular micelles because of many bearing side chains, which can be self-associated to form micelle core. Furthermore, graft copolymers with complicated architectures can lead to various possible associated structures [16–21]. In most cases, graft copolymers can form spherical micelles with core–shell structure in selective solvents. The micelles can be depicted as a core composed of lyophobic components surrounded with an outer shell composed of lyophilic components. In addition, graft copolymers have the advantage of lower critical aggregation concentrations than the surfactants with low molecular weight and block copolymers with the similar components, and the resulted micelles can be either unimolecular or multimolecular micelles [22–25]. However, the investigation on the self-assembly of the graft copolymers is still rather limited compared to the numerous works published on block copolymers [13,16,26–28], which is may be due to the difficulty in the controllable synthesis of well-defined graft copolymer during the past decades.

Cellulose is one of the abundant natural polymers which has the advantages of renewable, biodegradable and biocompatible properties. Cellulose and its derivatives are quite attractive for both academic and industrial researchers. However, cellulose cannot be melted and dissolved in normal organic solvent because of the strong inter- and intra-molecular hydrogen bonds. Therefore, the chemical modifications of cellulose have been studied extensively [29–31] and the grafting polymerization is one of the important modification of the cellulose. Cellulose graft copolymers have many potential utilities, for example they may be used in the target and controllable drug release system as the carrier materials [32,33]. More recently, atom transfer radical polymerization (ATRP) has been successfully used in the synthesis of cellulose graft copolymers with the well-defined chemical structure and new properties [34]. In our pervious works, a series of cellulose graft copolymers have been synthesized successfully [35,36] and it was found that the cellulose graft copolymers are able to self-assemble in selective

---

* Corresponding authors. State Key Laboratory of Polymer Physics and Chemistry, Joint Laboratory of Polymer Science and Materials, Beijing National Laboratory for Molecular Sciences (BNLMS), Institute of Chemistry, Chinese Academy of Sciences, Beijing 100190, China. Tel.: +86 10 82618573; fax: +86 10 62559373.

E-mail addresses: rgliu@iccas.ac.cn (R. Liu), yhuang@cashq.ac.cn (Y. Huang).

0032-3861/$ – see front matter © 2008 Elsevier Ltd. All rights reserved.
doi:10.1016/j.polymer.2008.10.060

solvents [37,38]. However, the relationship between the length of side chains for the graft copolymers and behavior of self-assembly of copolymer is not clear. In this work, therefore, the self-assembly of the dense graft copolymers, ethyl cellulose-*graft*-polystyrene (EC-*g*-PS), with different side-chain lengths in acetone was studied. Effects of the side-chain length and the copolymer concentration on the formation of the micelles for the EC-*g*-PS copolymers were discussed.

2. Experimental section

2.1. Materials

Ethyl cellulose (EC) (Luzhou Chemical Engineering Plant, Luzhou, China. $M_w = 4.7 \times 10^4$ g/mol and $M_w/M_n = 2.3$, determined by GPC), with a degree of ethyl substitution of 2.45 (determined by ^{1}H NMR), was used as received. The graft copolymers, ethyl cellulose-*graft*-polystyrene (EC-*g*-PS), were synthesized by atom transfer radical polymerization (ATRP) by using ethyl cellulose 2-bromoisobutyryl ester (EC-Br) as the macro-initiator of ATRP. The details of the synthetic procedure are shown elsewhere [35]. In the present work, the degree of substitution of 2-bromoisobutyryl of the macro-initiator EC-Br (DS_{Br}) was 0.5, which means that there was one initiating site for every two glucose rings and the resulted copolymer is dense graft copolymers.

The molar mass and its distribution of the graft copolymers were determined by gel permeation chromatography (GPC) (Waters 515 with a 2410 differential refractometer detector) with tetrahydrofuran (THF) as the eluting solvent (1 mL/min) and the monodisperse polystyrene was used as the standard. The composition of the copolymer was estimated by ^{1}H NMR spectra measured by a Bruker DMX 400 NMR spectrometer. The details of the structure of the cellulose graft copolymer are listed in Table 1.

2.2. Self-assembly of copolymers and characterization

EC is soluble and PS is relatively less soluble in acetone. The average hydrodynamic radius ($\langle R_h \rangle$) of EC is about 5 nm in acetone, which indicated that the ethyl cellulose is molecularly dissolved in acetone and no aggregation is formed. Therefore, acetone was chosen as a selective solvent to prepare EC-*g*-PS copolymer micelles in the solution.

The EC-*g*-PS copolymers were firstly dissolved in freshly distilled dichloromethane and the solution was stirred at room temperature overnight to ensure that the copolymer was completely dissolved. The resulted solution was then added dropwise into acetone with mild stirring. During the dropping procedure, the acetone solution turns into slightly bluish and then a little deep bluish with the continuous addition of the copolymer solution. The mixture was stirred for another several hours before the dichloromethane in the solution was evaporated under reduced pressure. The resulted solution with different copolymer concentrations was stored for the measurements.

Table 1
Molecular characteristics of the graft copolymers.

Copolymers	M_n[a] (g/mol)	M_w/M_n[a]	[Styrene]/ [glucose] molar ratio[b]	Average repeat units of the PS side chain[c]
G1	1.49×10^5	1.32	128	256
G2	1.34×10^5	1.38	81	162
G3	1.20×10^5	1.41	42	84
G4	1.13×10^5	1.47	10	20

[a] Parameter was determined by GPC.
[b] Molar ratio of average styrene unit and glucose unit was determined by ^{1}H NMR.
[c] Average number of styrene repeated unit of every PS graft was figured out by $DS_{Br} = 0.5$.

Dynamic light scattering (DLS) experiments were performed with a commercial spectrometer (ALV/SP-150), equipped with an ALV-5000 multi-τ digital time correlator and a solid-state laser (ADLAS DPY 425 II, output power was 400 mW at $\lambda = 632.8$ nm) was used as the light source. All DLS experiments were performed at 25 °C at the scattering angle of 90°. The apparent hydrodynamic radius (R_h) were obtained by fitting the correlation function with the CONTIN program.

Transmission electron microscopic (TEM) observation was carried out by using a Hitachi H-800 (Japan) transmission electron microscope at an acceleration voltage of 100 kV. The sample was prepared by dropping the copolymer solution (about 5 μL) on copper grids coated with carbon film and air dried.

Scanning electron microscopic (SEM) observation was performed by using a scanning electron microscope (JEOL 6700F, Japan). The samples for scanning electron microscopic observations

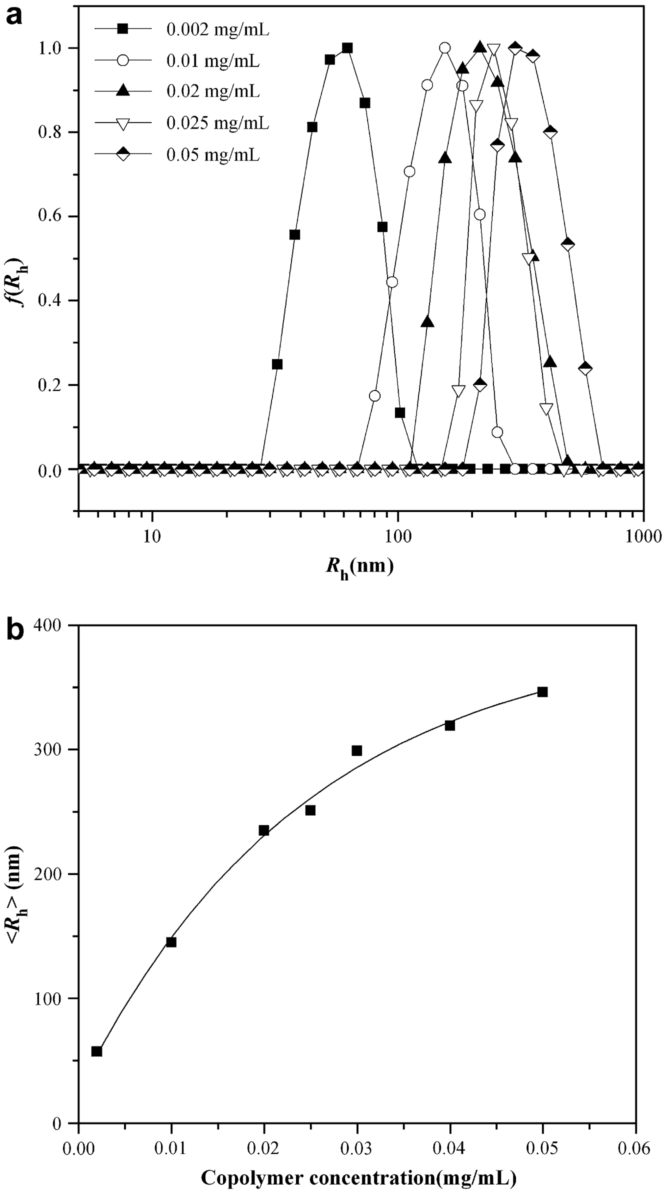

Fig. 1. Dependence of R_h on the concentration for the copolymer G1, (a) CONTIN plots of DLS data at different concentrations and (b) the average hydrodynamic radius ($<R_h>$) as a function of the concentration.

were prepared by placing about 5 μL of the copolymer solutions on freshly cleaned silicon wafers. The sample was then air dried one day and was observed by SEM after sputtering platinum.

3. Results and discussion

Fig. 1 shows the dependence of the hydrodynamic radius R_h of the micelles prepared from copolymer G1 on the copolymer concentration in the selective solvent of acetone. The average R_h ($\langle R_h \rangle$) is increased from 50 nm to 350 nm with increasing the copolymer concentration from 0.002 mg/mL to 0.05 mg/mL. The value of the hydrodynamic radius is much larger than that of a single chain, even at the lowest polymer concentration (0.002 mg/mL). This means that the graft copolymers in acetone are self-assembled into micelles. On the other hand, the large hydrodynamic radius in Fig. 1 suggests that the self-assembly of

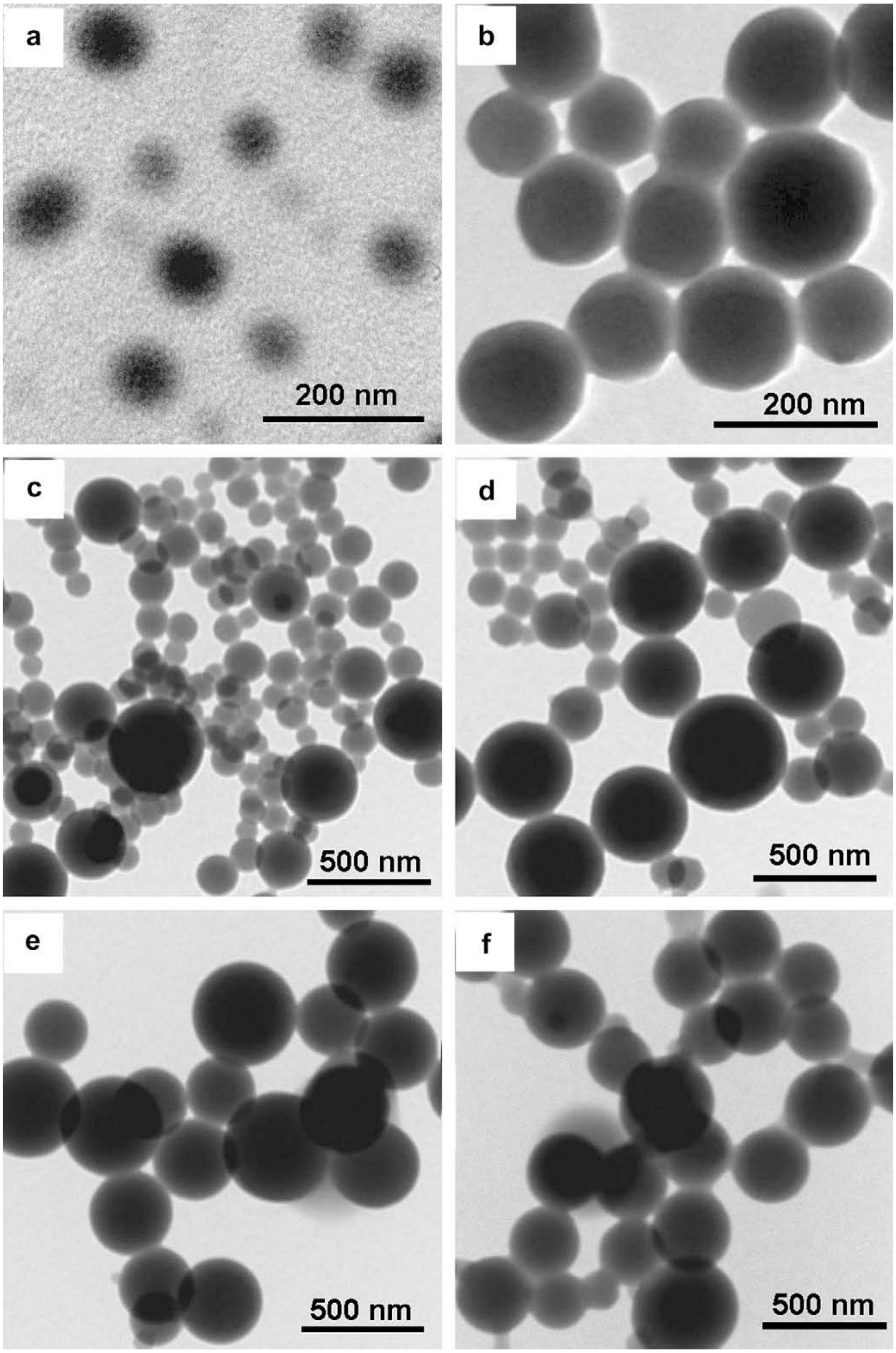

Fig. 2. TEM images of the micelles prepared from the G1 copolymer at different concentrations: (a) 0.002 mg/mL, (b) 0.01 mg/mL, (c) 0.025 mg/mL, (d) 0.03 mg/mL, (e) 0.05 mg/mL and (f) 0.1 mg/mL.

copolymers is a multimolecular assembly and the result of the inter-molecular association in acetone.

The typical TEM images of the micelles are shown in Fig. 2. It can be found from these images that the spherical micelles with core–shell structure are visible. When the concentration is 0.002 mg/mL, the diameter of the micelles is 20–100 nm (Fig. 2(a)). When the concentration is increased to 0.01 mg/mL, the diameter of the micelles is about 150 nm and the core–shell structure can be observed obviously (Fig. 2(b)). Increasing the concentration to 0.025 mg/mL, the micelles with a diameter of smaller than 200 nm are the majority but some micelles with the diameter of larger than 300 nm are also observed (Fig. 2(c)). Further increasing the concentration, micelles with the diameter of about 300 nm are more popular beside those with a smaller diameter (Fig. 2(d)). When the copolymer concentration is increased to 0.05 mg/mL, micelles with the diameter of about 300 nm are mainly observed (Fig. 2(e)). At a concentration of 0.1 mg/mL, only the micelles with a diameter around 320 nm are observed (Fig. 2(f)). The results show that the micelles' size is increased with increasing the copolymer concentration, which accorded with the DLS results. However, the average diameters of the micelles estimated by TEM images are smaller than those measured by DLS. This is due to that the micelles observed by TEM are collapsed after the evaporation of acetone, whereas the micelles are swollen in acetone during the DLS measurements. Moreover, the micelles with the diameter larger than 300 nm can be observed in the system prepared from the solution with the copolymer concentration of 0.025 mg/mL, which suggests that many copolymer chains have been simultaneously self-assembled to form large compound micelles [39]. It should be noted that the results obtained from DLS and TEM measurements are quite different. The TEM images show a bi-modal distribution of particle size (Fig. 2(c) and (d)), whereas the DLS experiments provide only the average value of R_h. This is due to that the DLS experiments provide the average value of the hydrodynamic radius ($\langle R_h \rangle$), while the hydrodynamic radius shows a broad distribution (Fig. 1(a)). Moreover, the range between the minimum and maximum of the hydrodynamic radius covers the particles' size observed in TEM images with the consideration of the collapse of the dried micelles.

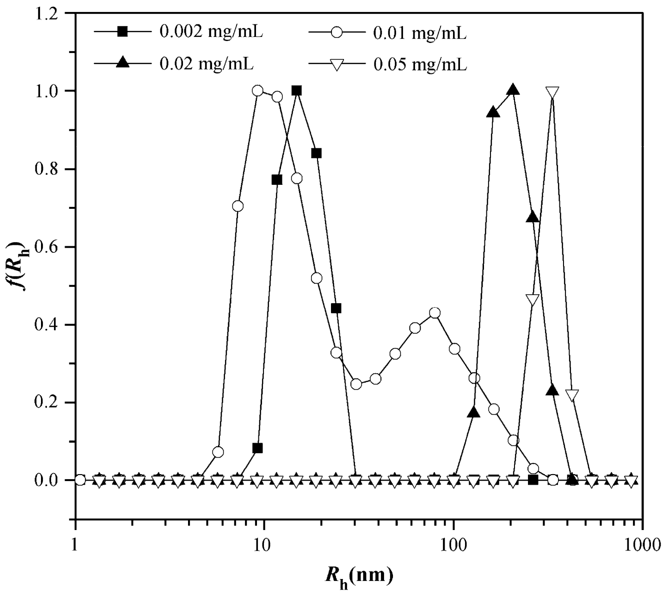

Fig. 4. Dependence of the hydrodynamic radius distribution on polymer concentration for the copolymer G2.

As mentioned before, dichloromethane is a good solvent for both the EC backbone and the PS side chains, while acetone is a good solvent only for EC backbone and a poor solvent for PS side chains. Therefore, it is suggested that the core of the EC-g-PS copolymer micelles in acetone is mainly composed of the PS side chains and the shell of the micelles is mainly composed of the EC backbone. The PS side chain has higher electron density than that of the EC backbone and so, the core of the micelles is darker than that of the shell in the TEM observation. In other words, the observed core–shell structure from the TEM images actually reflects the distribution of PS side chains and EC main chains. The composition of the core and the shell of micelles was further confirmed by SEM and TEM observation with staining of the sample. To enhance contrast between the core and the shell of copolymer micelles, osmium tetraoxide (OsO_4) and phosphotungstic acid (PTA) were used to stain the sample, respectively. After staining, the contrast between the core and the shell is enhanced obviously (Fig. 3). Fig. 3 clearly shows the micelles with spherical morphology and core–shell structure. It can be found from Fig. 3(b) that the core is darker than the shell when the sample is stained with OsO_4, which means that the core is mainly composed of the PS side chains because of reaction of OsO_4 with the carbon–carbon double bonds in PS side chains. However, the shell of the micelles is darker than the core when the sample is stained with PTA, which implies that the shell is mainly composed of the EC main chains because of adsorption of PTA the ester bonds in EC main chains [40]. The TEM observation with the sample stained by both OsO_4 and PTA suggests that the core of the micelles is mainly consisted of PS side chains, whereas

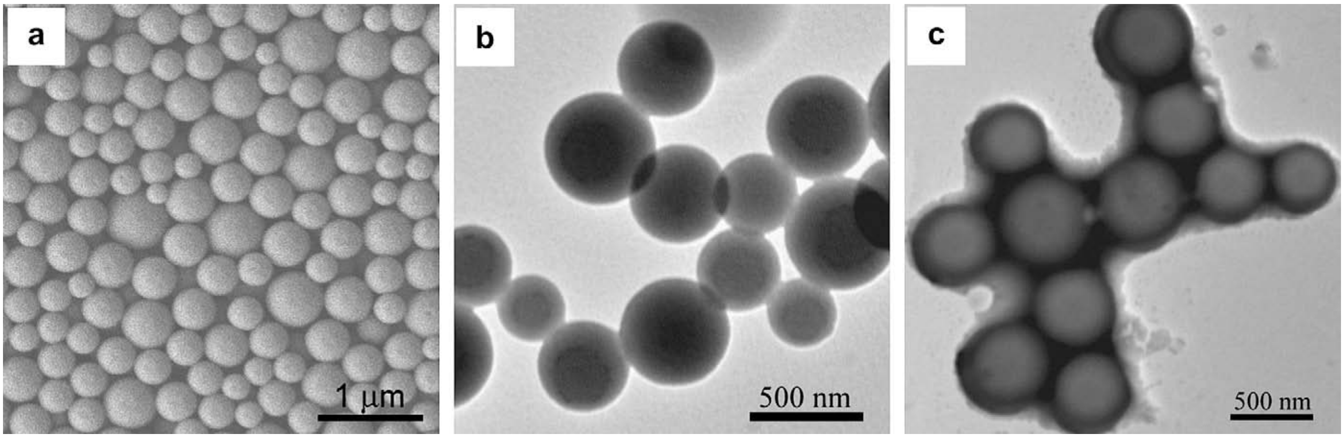

Fig. 3. Microscopic images of the micelles prepared from the G1 copolymer with copolymer concentration of 0.1 mg/mL: (a) SEM image, (b) TEM image with OsO_4 staining and (c) TEM image with PTA staining.

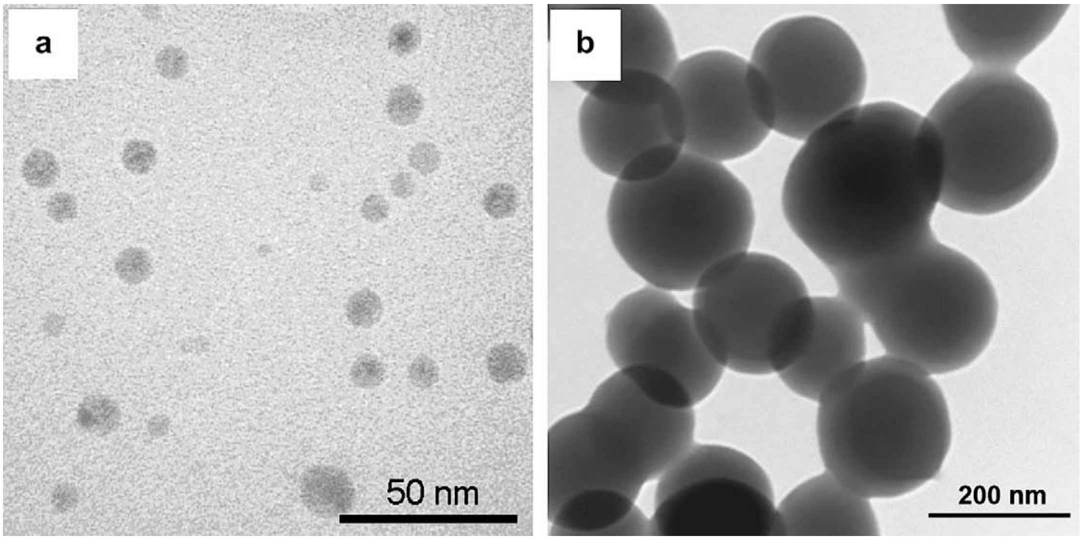

Fig. 5. Typical TEM images of the G2 copolymer at the copolymer concentration of (a) 0.002 mg/mL and (b) 0.05 mg/mL.

the shell of the micelles is mainly consisted of the EC main chains. Therefore, the copolymer micelles with core–shell structure in acetone were formed.

The hydrodynamic radius distribution of the micelles of copolymer G2, a copolymer with the shorter side chains than the copolymer G1, in acetone at different copolymer concentrations is shown in Fig. 4. Different from copolymer G1, the hydrodynamic radius ($\langle R_h \rangle$) is only about 11 nm when the copolymer concentration is only 0.002 mg/mL. This hydrodynamic radius value is slightly smaller than that of the single chain in a good solvent, which suggests that intra-molecular association occurs, and results in the formation of single molecular micelles at this concentration. The TEM observation also shows that the micelles of G2 are in the spherical morphology with the diameter in the range of 5–20 nm (Fig. 5(a)), which further confirmed the intra-molecular association. When the copolymer concentration is increased to 0.01 mg/mL, two peaks can be observed, corresponding to hydrodynamic radius of 10 nm and 80 nm (Fig. 4). This result suggests that intermolecular association occurs and multimolecular micelles are formed besides the intra-molecular association with the formation of unimolecular micelles. When the polymer concentration is further increased, the peak with the R_h of 10 nm disappears and only one peak can be observed, which is related to the intermolecular association. The results in Fig. 4 indicate, therefore, that copolymer G2 forms unimolecular micelles at low concentration ($\leq$0.002 mg/mL) and multimolecular micelles at the higher concentration ($\geq$0.01 mg/mL) in acetone. Unimolecular and multimolecular micelles of poly(methyl methacrylate)-*graft*-polystyrene (PMMA-*g*-PS) formed in selective solvents have also been observed [22,24].

In the case of copolymers G3 and G4 with even shorter PS side chains, the micellization or aggregation of the copolymers is more difficult than that of copolymers G1 and G2. Fig. 6 shows the typical TEM images for the copolymers G3 and G4 micelles formed in acetone at a concentration of 0.05 mg/mL. Different from the micelles of copolymers G1 and G2, the micelles of copolymers G3 and G4 formed in acetone are necklace-like by the junction of spherical micelles. The necklace-like micelles have been reported in the self-assembly of block copolymers and they are defined as the intermediate state between spherical and rod micelles, or the fusion of spherical micelles [1,41,42]. In EC-*g*-PS copolymers, acetone is used as the selective solvent, which is only a poor solvent for the PS side chains. Moreover, the shorter the PS side chain, the better the solubility of PS side chains in acetone, which leads to the intendance of the coupling of the PS side chains and the fusion of spherical micelles. Therefore, the formation of necklace-like morphology observed in the system of copolymers G3 and G4 is attributed to the fusion of the spherical micelles. The average diameters of the micelles estimated by TEM images are 130 nm and 60 nm for copolymers G3 and G4 at 0.05 mg/mL, respectively. Fig. 7 shows the dependence of the diameter of micelles, prepared in acetone with the concentration of 0.05 mg/mL, on the length of the PS side chains. The result in Fig. 7 indicates that the diameter of the micelles is increased with increasing the PS side-chain length. It is suggested, therefore, that the diameter of EC-*g*-PS copolymer micelles can be controlled by varying the length of the PS side

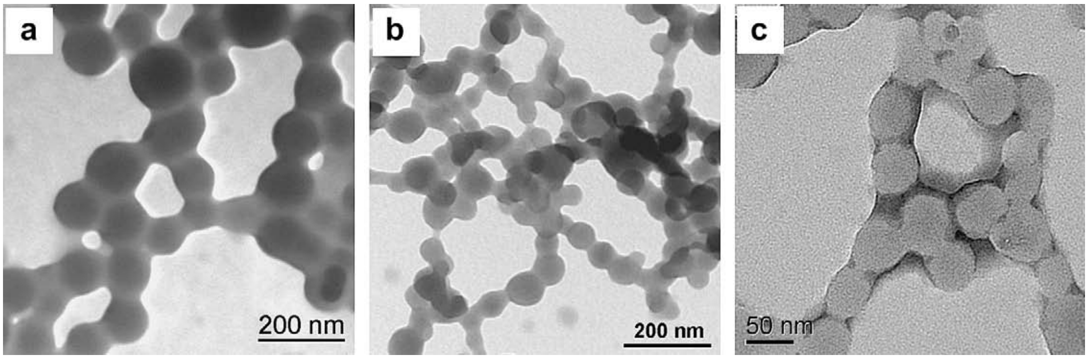

Fig. 6. TEM images of the micelles at a concentration of 0.05 mg/mL for the copolymers (a) G3, (b) G4 and (c) G4 with PTA staining.

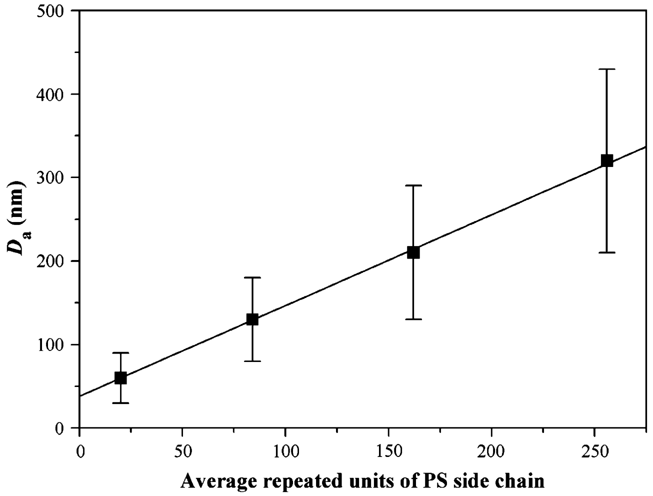

Fig. 7. Dependence of the micelles' size D_a on the average repeat unit of PS side chain. TEM results.

chains and it may provide a versatile method for changing the micelle size in the solution for graft copolymers.

It has been reported that the morphology of the micelles prepared from block copolymers can be influenced by the block length [43,44], whereas only spherical morphology was observed in this work. This is probably due to that the dense graft copolymers were used in this work. The dense graft polystyrene side chains lead to the strong lyophobic interaction, which is different from those of sparse graft copolymers [17]. The shorter side chain corresponds to the less lyophobic component and the more lyophilic component (the main EC chains), which can stabilize the micelles with a smaller size. Similar results had been reported for the block copolymers [45]. In this work, the micelles with core–shell structure can also be observed in the system of copolymers G2 and G3 (Figs. 5(b) and 6(a)). Whereas no clear core–shell structure was observed for the micelles prepared from the copolymer with the shortest side chain (G4). This is due to that the shorter PS side chain has a better compatibility with acetone, which leads to the less compact package of polystyrene side chains in the core of the micelles than those copolymers with a longer side chain. When the micelles prepared from G4 were stained by PTA, the core–shell structure can still be observed (Fig. 6(c)), which confirms that the EC main chains are rich in the outside layer of the micelles. In principle, the micelles prepared from copolymer G4 should have a thicker shell than those of the micelles prepared from G1–G3, due to that the PS content in the copolymer G4 is less than that of the other copolymers. However, only a thin shell can be observed in the micelles of G4, which suggests that there are some EC main chains in the core of the micelles prepared from the copolymer G4. The results indicate that the length of the side chains may change the assembly behavior of the EC-*g*-PS copolymers.

The EC-*g*-PS dense grafting copolymers are extended in dichloromethane which is a good solvent for both EC main chains and PS side chains. In acetone, which is a good solvent for EC main chains but a poor solvent for PS side chains, the PS side chains collapse and the copolymer self-assemble into micelles. When the polymer concentration is lower than the overlap concentration of the copolymers, the intra-molecular lyophobic interaction of the copolymer side chains leads to the formation of unimolecular micelles. The unimolecular micelles exhibit a single spherical morphology, which is different from that reported by Kikuchi and Nose [13]. Because the dense graft copolymer is used and the main chain is relatively rigid, the formation of loop or flower structures [13] is difficult, and the strong lyophobic interaction of the PS side chains promotes the formation of spherical structure. When the polymer concentration is increased to be higher than the overlap concentration of the copolymers, the inter-molecular association will result in the formation of multimolecular micelles. Further increasing the copolymer concentration, multimolecular micelles with larger size will be formed by molecular interaction with more polymer chains. Just like star copolymers, the multimolecular micelles may be a kind of multimolecular aggregates with the basic building units of unimolecular micelles, as reported by Hong et al. [15]. The large micelles may be connected together by lyophobic interaction of the PS side chains and necklace-like morphologies of the micelles are formed [46].

4. Conclusions

The self-assembly of EC-*g*-PS dense graft copolymers with different side-chain lengths in acetone was studied. It was found that the EC-*g*-PS copolymers can form spherical micelles with the core–shell structure in acetone. When the concentration is lower than the overlap concentration of the copolymers, unimolecular micelles are formed, whereas multimolecular micelles can be obtained when the concentration is higher than that. The unimolecular micelles and multimolecular micelles coexist in the system when the concentration is at about overlap concentration and the amount of the unimolecular micelles is decreased and that of the multimolecular micelles is increased with increasing the concentration. Moreover, the diameter of micelles is increased with increasing both the copolymer concentration and the side-chain length, which suggests that the size of the copolymer micelles can be controlled by both the concentration and the side-chain length of the graft copolymer.

Acknowledgements

The financial support by National Natural Science Foundation of China (Grant Nos. 20774105, 50521302) is greatly appreciated.

References

[1] Zhang LF, Yu K, Eisenberg A. Science 1996;272:1777–9.
[2] Zhang LF, Eisenberg A. J Am Chem Soc 1996;118:3168–81.
[3] Zhan YJ, Mattice WL. Macromolecules 1994;27:683–8.
[4] Zhu YT, Li RKY, Jiang W. Chem Phys 2006;327:137–43.
[5] Siddiq M, Hu HH, Ding MX, Li BZ, Wu C. Macromolecules 1996;29:7426–31.
[6] Bondzic S, Polushkin E, Ruokolainen J, ten Brinke G. Polymer 2008;49:2669–77.
[7] Tang XZ, Hu YH, Pan CY. Polymer 2007;48:6354–65.
[8] Gao JP, Wei YH, Li BY, Han YC. Polymer 2008;49:2354–61.
[9] Pispas S, Hadjichristidis N, Mays JW. Macromolecules 1996;29:7378–85.
[10] Inomata K, Yamamoto K, Nose T. Polym J 2000;32:1044–8.
[11] Mountrichas G, Mpiri M, Pispas S. Macromolecules 2005;38:940–7.
[12] Satoh T, Tamaki M, Kitajyo Y, Maeda T, Ishihara H, Imai T, et al. J Polym Sci Part A Polym Chem 2006;44:406–13.
[13] Kikuchi A, Nose T. Macromolecules 1996;29:6770–7.
[14] Lin JP, Zhu GQ, Zhu XM, Lin SL, Nose T, Ding WW. Polymer 2008;49:1132–6.
[15] Hong HY, Mai YY, Zhou YF, Yan DY, Cui J. Macromol Rapid Commun 2007;28:591–6.
[16] Zhang JX, Qiu LY, Zhu KJ. Macromol Rapid Commun 2005;26:1716–23.
[17] Wang CQ, Li GT, Guo RR. Chem Commun 2005:3591–3.
[18] Tanaka M, Fujita R, Nishide H. Polymer 2007;48:5884–8.
[19] Chan SC, Kuo SW, Lu CH, Lee HF, Chang FC. Polymer 2007;48:5059–68.
[20] Yang XM, Dai TY, Zhu ZX, Lu Y. Polymer 2007;48:4021–7.
[21] Tung PH, Kuo SW, Chen SC, Lin CL, Chang FC. Polymer 2007;48:3192–200.
[22] Kikuchi A, Nose T. Polymer 1996;37:5889–96.
[23] Wang XH, Xu ZD, Wan YN, Huang TZ, Pispas S, Mays JW, et al. Macromolecules 1997;30:7202–5.
[24] Kikuchi A, Nose T. Macromolecules 1997;30:896–902.
[25] Zhang Y, Lam YM, Tan WS. J Colloid Interface Sci 2005;285:74–9.
[26] Itakura M, Inomata K, Nose T. Polymer 2001;42:9261–8.
[27] Qiu XP, Wu C. Macromolecules 1997;30:7921–6.
[28] Dou HJ, Jiang M, Peng HS, Chen DY, Hong Y. Angew Chem Int Ed 2003;42:1516–9.
[29] Wang CQ, Dong YP, Tan HM. J Polym Sci Part A Polym Chem 2003;41:273–80.
[30] Roy D, Guthrie JT, Perrier S. Macromolecules 2005;38:10363–72.

[31] Yuan WZ, Yuan JY, Zhang FB, Xie XM. Biomacromolecules 2007;8:1101–8.
[32] Dou H, Jiang M. Polym Int 2007;56:1206–12.
[33] Tian Z, Wang M, Zhang AY, Feng ZG. Polymer 2008;49:446–54.
[34] Ostmark E, Harrisson S, Wooley KL, Malmstrom EE. Biomacromolecules 2007;8:1138–48.
[35] Shen DW, Yu H, Huang Y. J Polym Sci Part A Polym Chem 2005;43:4099–108.
[36] Shen DW, Yong H. Polymer 2004;45:7091–7.
[37] Kang H, Liu W, He B, Shen D, Ma L, Huang Y. Polymer 2006;47:7927–34.
[38] Kang H, Liu W, Liu R, Huang Y. Macromol Chem Phys 2008;209:424–30.
[39] Zhang LF, Eisenberg A. Science 1995;268:1728–31.
[40] Sawyer LC, Grubb DT. Polymer microscopy. London: Chapman & Hall; 1996.
[41] Adams DJ, Butler MF, Weaver AC. Langmuir 2006;22:4534–40.
[42] Terreau O, Luo LB, Eisenberg A. Langmuir 2003;19:5601–7.
[43] Shen HW, Eisenberg A. Macromolecules 2000;33:2561–72.
[44] Ibarboure E, Papon E, Rodriguez-Hernandez J. Polymer 2007;48:3717–25.
[45] Choucair A, Lavigueur C, Eisenberg A. Langmuir 2004;20:3894–900.
[46] Liu F, Frere Y, Francois J. Polymer 2001;42:2969–83.